Dyes and Pigments 105 (2014) 41–46

Contents lists available at ScienceDirect

Dyes and Pigments

journal homepage: www.elsevier.com/locate/dyepig

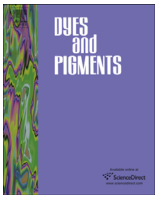

The third-order nonlinear optical properties of charge flowable trimethine cyanine with quinolone groups

Jia-Tao Miao [a], Xing-Zhi Wu [b], Ru Sun [a,]**, Ying-Lin Song [b], Jian-Feng Ge [a,]*

[a] College of Chemistry, Chemical Engineering and Material Science, Soochow University, 199 Ren'Ai Road, Suzhou 215123, China
[b] Department of Physics, Harbin Institute of Technology, Harbin 150001, China

ARTICLE INFO

Article history:
Received 4 December 2013
Received in revised form
10 January 2014
Accepted 15 January 2014
Available online 28 January 2014

Keywords:
Functional dyes
Optical property
Third-order nonlinear material
Z-scan
Optical material
Trimethine cyanine

ABSTRACT

Organic molecules with charge flow abilities gain much attention in third-order nonlinear optical materials. To evaluate the hypothesis of terminal donor and/or acceptor groups participating organic resonance structures for third-order nonlinear optical materials, conjugated double bonds structures with terminal amino groups are selected in this paper. The trimethine cyanine dye with quinolone skeleton (**3a**) was synthesized, it shows strong reverse saturable absorption and nonlinear refraction in dimethyl formamide solution at 532 nm. Then, its derivative compound (**3b**) with long alkyl chains was synthesized in order to improve the film forming performance, the spinning coating thin film exhibits strong reverse saturable absorption with the third-order nonlinear susceptibilities $\chi_I^{(3)} = 3.42 \times 10^{-8}$ esu and $\chi^{(3)} = 3.23 \times 10^{-9}$ esu under nanosecond and picosecond laser beams respectively. The results validate that the organic compounds with terminal donor and/or acceptor groups participating resonance structures have potential value for the design of the third-order nonlinear optical materials.

© 2014 Elsevier Ltd. All rights reserved.

1. Introduction

Organic third-order nonlinear optical (NLO) materials have gained much attention for their relatively large nonlinearities, fast response time and structural flexibility [1–3]. In the last two decades, there is no unique rule for the selection of organic third-order NLO materials, the design of them used to focus on the donor and/or acceptor linked conjugated structures [4–9], and the organic structures with charge flowability, such as diradical and zwitterionic compounds [10], were recently suggested as the key structures in this field.

Through a careful investigation of the reported organic third-order NLO materials, it is found that organic compounds with terminal donor and/or acceptor groups participating stable resonance structures would be good candidates for the requirements of charge flowable structures; for example, the structures of NIR dye of **BM4i4i** [11,12] and selenium containing cyanine dyes [13] are fit to above structural characteristics. In our previous work, aromatic heterocycles with amino groups were evaluated for the third-order NLO properties based on above hypothesis, phenoxazinium dyes exhibit strong third-order NLO reverse saturable absorptions and nonlinear refractions, and the effective third-order nonlinear susceptibilities ($\chi^{(3)}$) are up to 8.78×10^{-11} esu and 4.20×10^{-12} esu in acetonitrile solutions under nanosecond and picosecond laser Z-scan [14], meanwhile phenothiazinium dyes show similar third-order NLO properties with $\chi^{(3)}$ values being 5.16×10^{-11} esu and 3.40×10^{-12} esu under nanosecond and picosecond laser beams respectively [15]. The third-order NLO properties of two types fused heterocycles indicate the terminal donor and/or acceptor groups participating resonance structures would be good candidates in this field, however, more proofs with other type of conjugated systems are needed to affirm the hypothesis.

In this paper, the third-order NLO properties of the trimethine cyanine dyes, which have conjugated double bonds with terminal amino groups in quinolone, are reported in terms of their solution and films.

2. Experimental section

2.1. Materials

Starting materials and reagents (analytical grade) were purchased from TCI Development Co., Ltd. (Shanghai branch, China) or Sinopharm Chemical Reagent Co., Ltd. (Shanghai, China) and used

---

* Corresponding author. Tel./fax: +86 (0) 512 6588 4717.
** Corresponding author.
E-mail addresses: sunru924@hotmail.com (R. Sun), ge_jianfeng@hotmail.com (J.-F. Ge).

0143-7208/$ – see front matter © 2014 Elsevier Ltd. All rights reserved.
http://dx.doi.org/10.1016/j.dyepig.2014.01.014

directly. Chromatography was performed with silica gel (200–300 mesh).

2.2. Instruments

Melting points were determined on an X–4 microscope electron thermal apparatus (Taike, China) and the values are uncorrected. NMR spectra were recorded on a Varian-300 or 400 MHz spectrometer. Mass spectra were recorded on Finnigan MAT95 mass spectrometer. UV–vis absorption spectra were recorded on a Shimadzu U–3900 spectrometer. Atomic force microscope (AFM) images were tested with a Bruker dimension icon system. The thickness of the films was obtained by a Hitachi S–4700 scanning electron microscope (SEM).

The third-order NLO properties were measured by the Z-scan technique as reported method [16,17], laser pulses at wavelength of 532 nm with pulse width of 4 ns (fwhm) were generated from a frequency–doubled and Q-switched Nd:YAG laser and an Nd:YAG 532 nm laser (EKSPLA) with a pulse width of 21 ps (fwhm) and repetition rate of 10 Hz was used for picosecond measurements.

2.3. Synthesis

2.3.1. Synthesis of 1-ethyl-4-methylquinolin-1-ium iodide (*1a*) and 1-ethyl-4-(2-(N-phenyl- acetamido)vinyl)quinolin-1-ium iodide (*2a*)

Compounds **1a** and **2a** were prepared according to the reported procedures [18].

2.3.2. Synthesis of 1-decyl-4-methylquinolin-1-ium iodide (*1b*)

A solution of 4-methylquinoline (2.00 g, 14.0 mmol) and 1-iododecane (4.50 g, 16.8 mmol) in acetonitrile (140 mL) was refluxed for 48 h under nitrogen atmosphere. The solvent was removed under reduced pressure and the residue was purified by column chromatography eluting with dichloromethane and acetone (v:v = 2:1) to give the brown liquid product. Yield: 51.5%; ^{1}H NMR (400 MHz, $CDCl_3$) δ 10.15 (d, J = 6.0 Hz,1H, Ar–H), 8.39 (d, J = 8.7 Hz, 2H, 2 × Ar–H), 8.30–8.15 (m, 2H, 2 × Ar–H), 8.04 (d, J = 6.1 Hz, 1H, Ar–H), 8.01 (dd, J = 8.2, 7.3 Hz, 1H, Ar–H),, 5.27 (t, J = 7. Hz, 2H, CH_2), 3.03 (s, 3H, CH_3), 2.17–2.02 (m, 2H, CH_2), 1.56–1.45 (m, 2H, CH_2), 1.40–1.31 (m, 2H, CH_2), 1.31–1.18 (m, 10H, 5 × CH_2), 0.86 (t, J = 6. Hz, 3H, CH_3). ^{13}C NMR (75 MHz, $CDCl_3$) δ 158.34, 148.43, 136.99, 135.86, 130.26, 129.49, 127.14, 123.20, 119.17, 58.15, 31.78, 30.22, 29.44, 29.34, 29.19, 29.13, 26.49, 22.60, 20.87, 14.09. MS (ESI$^+$) m/z: calcd for $C_{20}H_{30}N^+$: 284.2378, found: 284.2378 [M-I$^-$]$^+$.

2.3.3. Synthesis of 1-decyl-4-(2-(N-phenylacetamido)vinyl) quinolin-1-ium iodide (*2b*)

Compound **1b** (1.65 g, 4.0 mmol) was reacted with N,N′-diphenylformamidine (0.79 g, 4.0 mmol) at 165 °C for 30 min, the residue product was washed with diethyl ether and ethanol sequentially, then dried under reduced pressure. Acetic anhydride (3 mL) and triethyl orthoformate (1.5 mL) were added to the above residue and the resultant suspension was stirred at 100 °C for 15 min. The reactant was cooled to room temperature, diethyl ether (20 mL) was added slowly. The product was collected by filtration and finally purified by column chromatography eluting with dichloromethane and acetone (v:v = 2:1) to give the product as a yellow solid. Yield: 30.6%; mp 143.2–144.5 °C; ^{1}H NMR (400 MHz, $CDCl_3$) δ 9.90 (d, J = 6.3 Hz, 1H, Ar–H), 8.88 (d, J = 14.1 Hz, 1H, Ar–H), 8.19 (d, J = 8.8 Hz, 1H, Ar–H), 8.16–8.02 (m, 2H, 2 × Ar–H), 7.88 (d, J = 8.5 Hz, 1H, CH), 7.76 (t, J = 7.7 Hz, 1H, Ar–H), 7.66 (m, J = 14.4, 7.3 Hz, 3H, 3 × Ar–H), 7.37 (d, J = 7.3 Hz, 2H, 2 × Ar–H), 6.02 (d, J = 14.1 Hz, 1H, CH), 5.12 (t, J = 7.4 Hz, 2H, CH_2), 2.09 (s, 3H, CH_3), 2.03 (m, 2H, CH_2), 1.55–1.40 (m, 3H, CH_3), 1.33 (m, J = 5.7 Hz, 2H, CH_2), 1.23 (s, 10H, 5 × CH_2), 0.86 (t, J = 6.5 Hz, 3H, CH_3). ^{13}C NMR (75 MHz, $CDCl_3$) δ 169.80, 153.87, 147.38, 140.66, 137.77, 135.40, 131.09, 130.32, 129.16, 128.31, 126.51, 125.79, 118.71, 115.18, 103.54, 57.38, 31.80, 30.00, 29.30, 26.51, 23.60, 22.63, 14.11. MS (ESI$^+$) m/z: calcd for $C_{29}H_{37}N_2O^+$: 429.2906, found: 429.2892 [M-I$^-$]$^+$.

2.3.4. Synthesis of 1-ethyl-4-(3-(1-ethylquinolin-4(1H)-ylidene) prop-1-en-1-yl)quinolin-1-ium iodide (*3a*)

To a mixture of **2a** (201.0 mg, 0.5 mmol) and **1a** (149.5 mg, 0.5 mmol) in ethanol (5 mL), Et_3N (0.15 mL) was added in portions, and then the mixture was refluxed for 1 h. The reactant was cooled to room temperature; the product was separated by filtration and recrystallized from methanol to give dark green powder. Yield: 42.5%, mp 248.3–250.2 °C; ^{1}H NMR (400 MHz, DMSO) δ 8.70 (t, J = 13.0 Hz, 1H, CH), 8.38 (d, J = 8.4 Hz, 2H, 2 × Ar–H), 8.17 (d, J = 7.3 Hz, 2H, 2 × Ar–H), 7.93 (d, J = 8.7 Hz, 2H, 2 × Ar–H), 7.85 (t, J = 7.7 Hz, 2H, 2 × Ar–H), 7.80 (d, J = 7.4 Hz, 2H, 2 × Ar–H), 7.60 (t, J = 7.6 Hz, 2H, 2 × Ar–H), 7.10 (d, J = 13.0 Hz, 2H, 2 × CH), 4.47 (q, J = 6.8 Hz, 4H, 2 × CH_2), 1.41 (t, J = 7.0 Hz, 6H, 2 × CH_3). ^{13}C NMR (151 MHz, DMSO) δ 148.30, 142.51, 140.28, 137.71, 132.61, 125.74, 124.86, 124.13, 117.15, 110.40, 108.71, 48.35, 14.47. MS (ESI$^+$) m/z: calcd for $C_{25}H_{24}N_2^+$: 353.2018, found: 353.2017 [M-I$^-$]$^+$.

2.3.5. Synthesis of 1-decyl-4-(3-(1-decylquinolin-4(1H)-ylidene) prop-1-en-1-yl)quinolin-1-ium iodide (*3b*)

To a mixture of **2b** (278.2 mg, 0.5 mmol) and **1b** (205.6 mg, 0.5 mmol) in ethanol (5.0 mL), Et_3N (0.15 mL) was added in portions, and then the mixture was refluxed for 1 h. The reactant was cooled to room temperature, and ethyl ether (30 mL) was added. The product was collected by filtration and purified by column chromatography eluting with dichloromethane and acetone (v:v = 2:1) to give the target product as a dark green solid. Yield: 58.5%. mp 155.1–156.0 °C. ^{1}H NMR (400 MHz, $CDCl_3$) δ 8.41 (t, J = 12.9 Hz, 1H, CH), 8.23 (d, J = 8.2 Hz, 2H, 2 × Ar–H), 7.79 (d, J = 7.3 Hz, 2H, 2 × Ar–H), 7.73 (d, J = 7.5 Hz, 2H, 2 × Ar–H), 7.66 (t, J = 7.8 Hz, 2H, 2 × Ar–H), 7.49 (d, J = 8.7 Hz, 2H, 2 × Ar–H), 7.44 (t, J = 7.5 Hz, 2H, 2 × Ar–H), 6.86 (d, J = 13.0 Hz, 2H, 2 × CH), 4.18 (t, J = 7.3 Hz, 4H, 2 × CH_2), 1.87–1.73 (m, 4H, 2 × CH_2), 1.45–1.12 (m, 28H, 14 × CH_2), 0.86 (t, J = 6.8 Hz, 6H, 2 × CH_3). ^{13}C NMR (75 MHz, $CDCl_3$) δ 148.73, 142.46, 140.08, 137.97, 132.32, 125.55, 124.75, 116.19, 110.69, 109.97, 54.45, 31.84, 29.48, 29.44, 29.25, 29.23, 29.11, 26.74, 22.66, 14.11. MS(ESI$^+$) m/z: calcd for $C_{41}H_{57}N_2^+$: 577.4522, found: 577.4531 [M-I$^-$]$^+$.

2.4. Spinning coating of the film

The quartz glass (25 × 25 × 1 mm^3) was sequentially washed with distilled water, acetone, ethanol and then acetone in an ultrasonic bath. Dye **3b** (20.0 mg) was dissolved in cyclopentanone (1.0 mL). The solution, which was filtered through a 0.22 μm filter, was subsequently spin–coated at 1300 rmp on a quartz glass and the film was dried in a vacuum oven at 60 °C for 24 h to remove the residual solvent.

3. Results and discussion

3.1. Preparation of the materials

The synthetic schedule is shown in Fig. 1. Compounds **1a–b** were synthesized by the alkylation of the 4-methylquinoline. The intermediates (**2a–b**) can be obtained by the one [19] or two steps [18] synthesis according to the reported methods, and the two steps synthesis was adopted for **2a–b** since the procedures are more efficient for purification in this case. The final products (**3a–b**) were prepared by the condensations between the **2a**–2**b** and

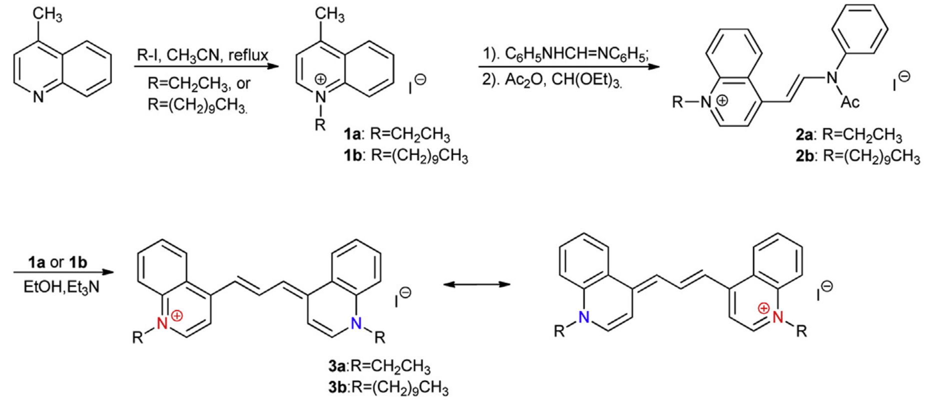

Fig. 1. Synthetic routes of trimethine cyanine dyes with quinolones.

1a–**1b** respectively with the triethylamine as base. The decomposition temperature of **3a**–**3b** is up to 270–280 °C (Fig. S1), which indicates the thermal stability of the cyanine dyes. The structures of **3a**–**3b** consist of two stable resonance structures and terminal nitrogen atoms participating the resonance skeletons, these features are well fit to the suggested hypothesis of the organic charge flowable structures for third-order NLO materials.

3.2. Optical properties of compound **3a** in DMF

The normalized absorption spectrum of **3a** in dimethyl formamide (DMF) solution was shown in Fig. 2 (**3a** in DMF), it has absorption maximum at 712 nm with a shoulder peak at 657 nm, which could identify the *H*-aggregation of the cyanine dye in the solution [20]. The solution has no absorption at 532 nm, so the third-order NLO properties could be measured with the 532 nm laser beam without the influence from linear absorption comparing with the reported third-order NLO properties of the cyanine dyes [21,22].

The third-order NLO properties of compound **3a** were tested by Z-scan with nanosecond laser beam at 532 nm. The DMF solution of **3a** shows strong reverse saturable absorption (RSA) and nonlinear refraction (Figs. S2 and S3) with the third-order nonlinear susceptibilities $\chi_R^{(3)} = 1.45 \times 10^{-11}$ esu, $\chi_I^{(3)} = 2.08 \times 10^{-11}$ esu and $\chi^{(3)} = 2.54 \times 10^{-11}$ esu which can be calculated by the reported methods [23,24] (Table S1). The remarkable third-order NLO properties of compound **3a** show the potential application of the terminal nitrogen atoms participating resonance structure of trimethine cyanine, unfortunately, compound **3a** is difficult to form a thin film because of its undesirable physical characteristics. Thus the design of derivatives of **3a** is necessary for the third-order NLO properties in solution as well as thin film.

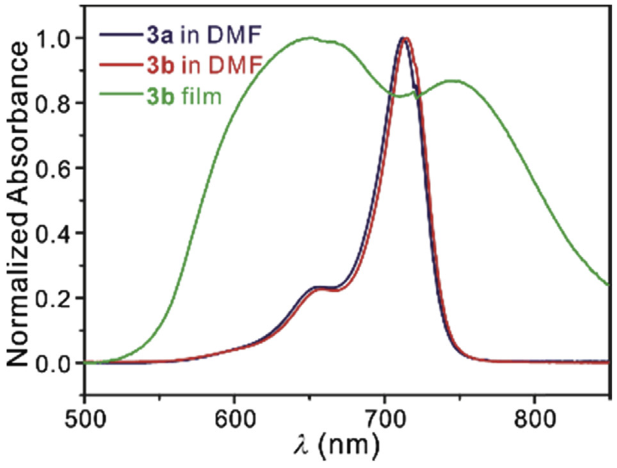

Fig. 2. Normalized absorption spectra of **3a**–**3b**.

3.3. Optical properties of compound **3b** in DMF solution and film

The spin-coating method was reported as the easy way to form optical thin films, and that functional dyes with long alkyl chains

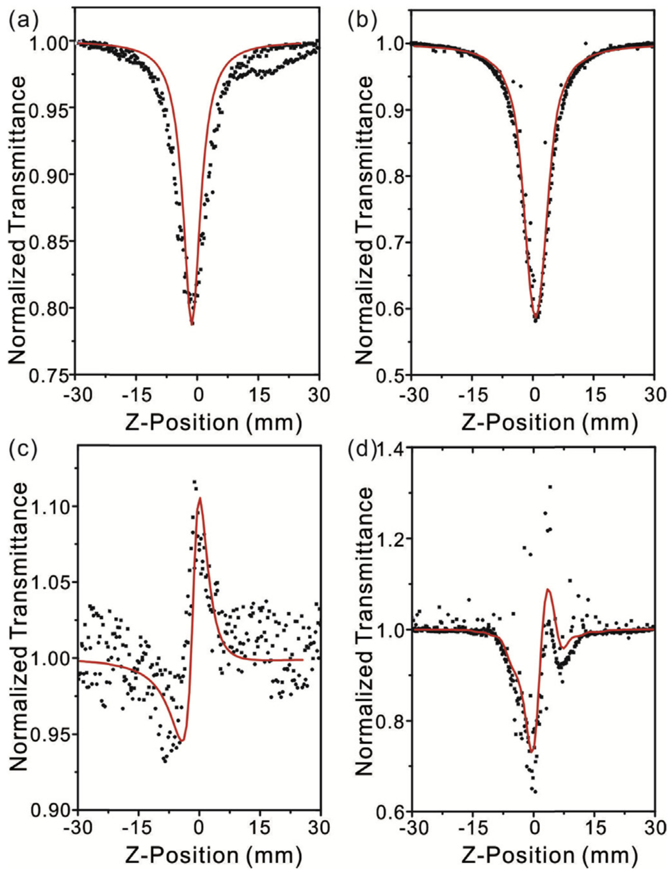

Fig. 3. Third-order NLO responses of compound **3b** (1.0×10^{-3} mol L^{-1}) in DMF solution (points are tested data and lines are fit curves). (a) and (b): open aperture transmittances; (c) and (d): refractive parts, data were obtained from the ratio of the closed aperture transmittance divided by the open aperture transmittance. (a) and (c): tested with nanosecond laser beam at 532 nm; (b) and (d): tested with picosecond laser beam at 532 nm.

Table 1
The third-order NLO properties of the compound **3b**.

Entry	Samples	Laser	T_0[a]	n_2 ($m^2 W^{-1}$)[b]	β ($m W^{-1}$)[c]	$\chi_R^{(3)}$ (esu)[d]	$\chi_I^{(3)}$ (esu)[e]	$\chi^{(3)}$ (esu)[f]	γ' (esu)[g]
1	**3b** in DMF[h]	ns[i]	0.72	8.50×10^{-17}	1.50×10^{-9}	3.08×10^{-11}	3.29×10^{-11}	4.51×10^{-11}	2.26×10^{-32}
2	**3b** Film	ns[j]	0.86	–	1.80×10^{-6}	–	3.42×10^{-8}	–	–
3	**3b** in DMF[h]	ps[k]	0.71	3.40×10^{-18}	1.31×10^{-10}	1.23×10^{-12}	2.87×10^{-12}	3.12×10^{-12}	1.56×10^{-33}
4	**3b** Film	ps[k]	0.86	8.70×10^{-15}	9.10×10^{-8}	2.73×10^{-9}	1.73×10^{-9}	3.23×10^{-9}	1.91×10^{-31}

[a] Linear transmittance.
[b] Nonlinear refractive index.
[c] Nonlinear absorption coefficient.
[d] Real part of third-order nonlinear susceptibility.
[e] Imaginary part of third-order nonlinear susceptibility.
[f] Third-order nonlinear susceptibility.
[g] Second-order hyperpolarizability.
[h] With the concentration at 1.0×10^{-3} mol L^{-1}.
[i] Tested with nanosecond laser beam (532 nm) at 1.20 μJ.
[j] Tested with nanosecond laser beam (532 nm) at 0.90 μJ.
[k] Tested with picosecond laser beam (532 nm) at 0.25 μJ.

[25], composite materials [26–30], side-chain polymers [31,32] and sol–gel complexes [33,34] were used for the film. Functional dye with decyl groups was selected for derivative of the trimethine cyanine, and compound **3b** was obtained by altering the substituent group of **3a** to improve the film-forming ability (Fig. 1). The linear optical absorption of **3b** in DMF (Fig. 2, **3b** in DMF), absorption maximum at 714 nm with a shoulder peak at 658 nm, is similar to that of **3a**.

The third-order NLO properties of **3b** (1.0×10^{-3} mol L^{-1}) in DMF were firstly evaluated by Z-scan with 532 nm nanosecond laser beam at 1.20 μJ. The third-order NLO absorption was expressed by open aperture transmittance as shown in Fig. 3(a), and the solution shows strong RSA. The nonlinear refractive data were obtained from the closed aperture transmittance divided by the open aperture transmittance, and the valley-to-peak configuration of the curve suggests self-focusing effect (Fig. 3(c)). The calculated third-order NLO parameters are $\chi^{(3)} = 4.51 \times 10^{-11}$ esu, second-order hyperpolarizability $\gamma\prime = 2.26 \times 10^{-32}$ esu (Table 1, Entry 1). Strong third-order NLO RSA and refractive phenomena with $\chi^{(3)} = 3.12 \times 10^{-12}$ esu and $\gamma\prime = 1.56 \times 10^{-33}$ esu were also verified by the 532 nm picosecond laser beam at 0.25 μJ (Fig. 3 (b) and (d); Table 1, Entry 3). Comparing with the reported properties of pentamethine cyanine [35], compound **3b** has the similar third-order NLO performance in the same test condition although it has shorter conjugated double bond skeleton, and the results also indicate the importance of the terminal nitrogen atoms participating the resonance skeletons for third-order NLO materials.

The optical film of **3b** was prepared by spin coating. The film has the smooth surface (Fig. 4(a)) with waviness of the topographic at about 2 nm (Fig. 4(c)). The cross-sectional SEM image reveals that the thickness of the film is 144 nm (Fig. 4(b)). These material features of the film with **3b** indicate the long alkyl chains of decyl groups are good selection for optical device of the trimethine cyanine. The absorption spectra of the film containing **3b** is shown in Fig. 2 (**3b** film), the absorption maximum locates at 651 nm with a shoulder band at 745 nm, the difference between the absorptions of **3b** in solution and film would be induced by the existent of *J* and *H*-aggregations for the cyanine dye at the same time [36].

Strong RSA of the film was found by the Z-scan with nanosecond laser beam with 532 nm at 0.90 μJ (Fig. 5(a)), and that the imaginary part of third-order nonlinear susceptibility is up to 3.42×10^{-8} esu (Table 1, Entry 2); the refractive part cannot be detected under this condition (Fig. 5(c)) due to the strong RSA in this condition. Meanwhile, strong RSA and nonlinear refraction phenomena were observed by picosecond laser beam with 532 nm at 0.25 μJ (Fig. 5(b) and (d)), and it has remarkable third-order NLO parameter with $\chi^{(3)} = 3.23 \times 10^{-9}$ esu and $\gamma\prime = 1.91 \times 10^{-31}$ esu. The third-order properties of compound **3a** and **3b** affirm the hypothesis for

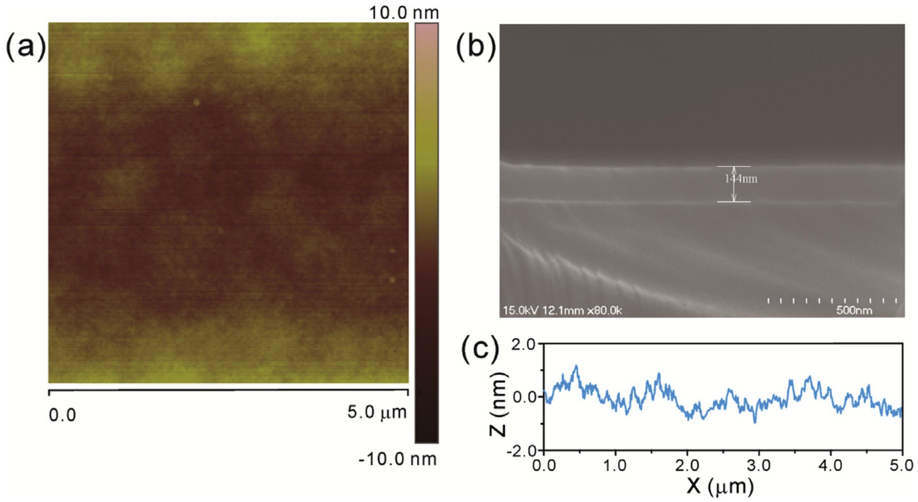

Fig. 4. Characteristics of the spin-coating film. (a): AFM height image of the film; (b): SEM image of the film cross section; (c): a typical cross section profile of AFM topographic image.

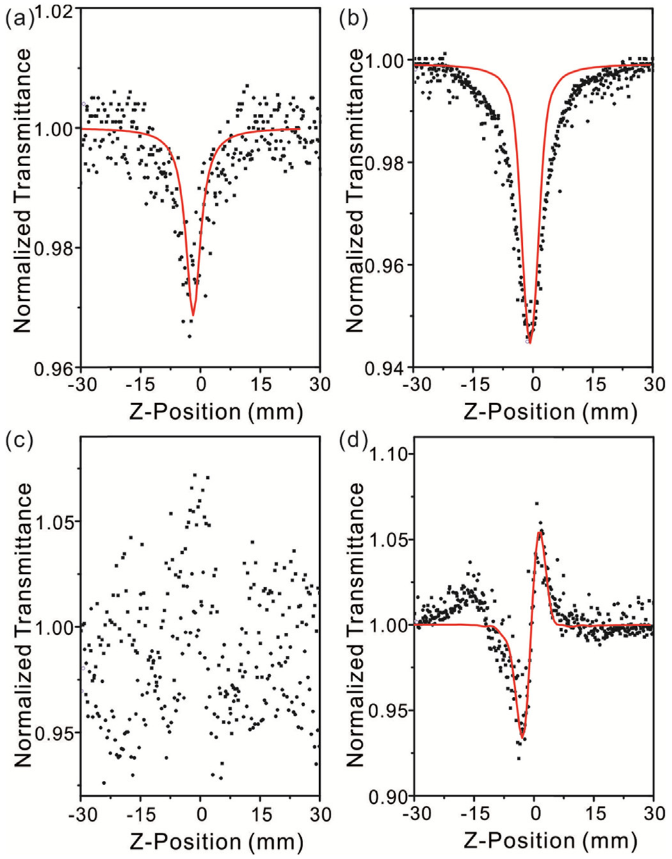

Fig. 5. Third-order NLO responses of spin-coating film with **3b** (points are tested data and lines are fit curves). (a) and (b): open aperture transmittances; (c) and (d): refractive parts, data were obtained from the ratio of the closed aperture transmittance divided by the open aperture transmittance. (a) and (c): tested with nanosecond laser beam at 532 nm; (b) and (d): tested with picosecond laser beam at 532 nm.

selection of third-order NLO materials from terminal donor and/or acceptor groups containing stable resonance structures.

4. Theoretical calculations

To get insight into the optical properties of **3a**–**3b**, (TD)DFT calculations with the B3LYP exchange functional employing 6-311 + G(d) basis sets were performed with the Gaussian09 program package [37]. Solvent effects are considered by conductor-like polarizable continuum model (CPCM) and DMF is used as solvent. The optimized structures and molecular orbital plots of cations **3a**$^+$–**3b**$^+$ are shown in Fig. 6 and Figs. S4 and S5. Selected parameters for the vertical excitation (UV–vis absorptions) of them are displayed in Table S2.

The analysis of the wave function indicates that the electron absorption corresponds to the transition from the ground to the first excited state (S0 → S1) and is mainly described by one-electron excitation from the highest occupied molecular orbital (HOMO) to the lowest unoccupied orbital (LUMO)(Table S2). For both **3a**$^+$ and **3b**$^+$, the two quinoline rings are not in the same plane (Fig. S4), and the dihedral angles between which are 36° and 32° respectively. Even so, the HOMOs and LUMOs of **3a**$^+$–**3b**$^+$ are still delocalized over the whole conjugated structure, that is, the two quinoline chromophore and conjugated double bonds (Fig. S5, Fig. 6).

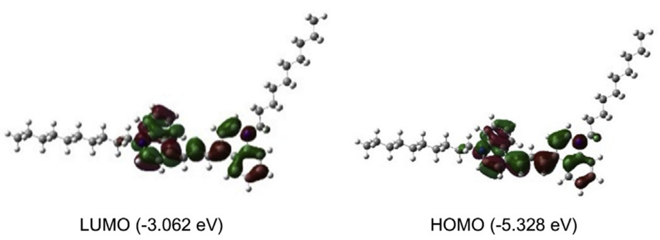

Fig. 6. The HOMO and LUMO of **3b**$^+$ in DMF.

NBO charge analysis shows the charges on two nitrogen atoms of **3a**$^+$ are −0.366e and −0.363e. However, for **3b**$^+$, the charges are −0.371e and −0.364e respectively. The two nitrogen atoms on the heterocyclic ring have a strong electron-withdrawing ability, and on both sides of the electron decyl group, it can effectively push the electronic nitrogen atom, to form a suction-supply system, and to enhance the degree of intramolecular charge transfer. This long electron conjugated structure for a suction system is present, so that the compound **3b** under the action of the light stronger electron–photon coupling, thus contributing to increasing the electron from the ground state to the excited state, reducing the transition energy from 2.269 eV for **3a**$^+$ to 2.266 eV for **3b**$^+$ (Figs. 6, S5), so the sample **3b** has a more strong third-order nonlinear optical response.

5. Conclusions

Due to the requirements of the organic third-order NLO materials, trimethine cyanine dyes with terminal donor and/or acceptor groups participating resonance structures were selected in this paper. 1-Ethyl-4-(3-(1-ethylquinolin-4(1H)-ylidene)prop-1-en-1-yl)quinolin-1-ium iodide (**3a**) shows strong reverse saturable absorption and nonlinear refraction by Z-scan under nanosecond laser beam at 532 nm, then the derivative compound, 1-decyl-4-(3-(1-decylquinolin-4(1H)-ylidene)prop-1-en-1-yl)quinolin-1-ium iodide (**3b**), with long alkyl groups was redesigned and synthesized. Optical film of **3b** can easily be prepared by spin-coating, and it exhibits more strong reverse saturable absorption at 532 nm, the imaginary part of third-order nonlinear susceptibility is up to 3.42 × 10^{-8} esu under nanosecond laser beam, and the nonlinear susceptibility is up to 3.23 × 10^{-9} esu under picosecond laser beam, respectively. Their optical properties are discussed through NBO charge distribution analysis and the frontier molecular orbital theory. The results of this research validate the potential application of the terminal donor and/or acceptor groups participating stable resonance structures in designing the third-order NLO materials.

Acknowledgments

The project is supported from the National Natural Science Foundation of China (51273136) and the Project funded by the Priority Academic Program Development of Jiangsu Higher Education Institutions.

Appendix A. Supplementary data

Supplementary data related to this article can be found at http://dx.doi.org/10.1016/j.dyepig.2014.01.014.

References

[1] Nalwa HS. Organic materials for third-order nonlinear optics. Adv Mater 1993;5:341–58.
[2] Kaino T, Tomaru S. Organic materials for nonlinear optics. Adv Mater 1993;5:172–8.

[3] Bredas JL, Adant C, Tackx P, Persoons A, Pierce BM. Third-order nonlinear optical response in organic materials: theoretical and experimental aspects. Chem Rev 1994;94:243–78.

[4] Rath H, Sankar J, PrabhuRaja V, Chandrashekar TK, Nag A, Goswami D. Core-modified expanded porphyrins with large third-order nonlinear optical response. J Am Chem Soc 2005;127:11608–9.

[5] Bucher C, Devillers C, Moutet J, Royal G, Saintaman E. Ferrocene-appended porphyrins: syntheses and properties. Coord Chem Rev 2009;253:21–36.

[6] Delaire JA, Nakatani K. Linear and nonlinear optical properties of photochromic molecules and materials. Chem Rev 2000;100:1817–46.

[7] Cifuentes MP, Humphrey MG, Morrall JP, Samoc M, Paul F, Lapinte C, et al. Third-order nonlinear optical properties of some electron-rich iron mono- and trinuclear alkynyl complexes. Organometallics 2005;24:4280–8.

[8] Mattu J, Johansson T, Leach GW. Third-order nonlinear optical response from polythiophene-based thin films. J Phys Chem C 2007;111:6868–74.

[9] Faccinetto A, Mazzucato S, Pedron D, Bozio R, Destri S, Porzio W. Non-resonant z-scan characterization of the third-order nonlinear optical properties of conjugated poly(thiophene azines). Chemphyschem Eur J Chem Phys Phys Chem 2008;9:2028–34.

[10] Prabhakar C, Yesudas K, Bhanuprakash K, Rao VJ, Santosh Kumar RS, Rao DN. Linear and nonlinear optical properties of mesoionic oxyallyl derivatives: enhanced non-resonant third order optical nonlinearity in croconate dyes. J Phys Chem C 2008;112:13272–80.

[11] Langhals H. An unexpectedly simple nir dye for 1.1 microm with a central mesoionic structure. Angew Chem 2003;42:4286–8.

[12] Tatsuura S, Matsubara T, Tian M, Mitsu H, Iwasa I, Sato Y, et al. Ultrafast all-optical switching at 1.55 μm using an organic multilayer device. Appl Phys Lett 2004;85:540.

[13] Hales JM, Matichak J, Barlow S, Ohira S, Yesudas K, Bredas JL, et al. Design of polymethine dyes with large third-order optical nonlinearities and loss figures of merit. Science 2010;327:1485–8.

[14] Ge J-F, Lu Y-T, Xu Q-F, Liu W, Li N-J, Sun R, et al. Third-order nonlinear optical properties of a new type of d–π–d unsymmetrical phenoxazinium chloride with resonance structures. Chem Phys 2011;382:74–9.

[15] Lu Y-T, Ge J-F, Xu Q-F, Yang Y, Li N-J, Sun R, et al. Third-order nonlinear optical properties of the phenothiazinium chlorides at 532 nm. Dyes Pigments 2011;89:70–5.

[16] Wang D, Zhang S, Zhang Y, Wang H, Mu J, Wang G, et al. Preparation and nonlinear optical characterization of a novel hyperbranched poly(aryl ether ketone) end-functionalized with nickel phthalocyanine. Dyes Pigments 2008;79:217–23.

[17] Chen X, Zhang J, Zhang H, Jiang Z, Shi G, Li Y, et al. Preparation and nonlinear optical studies of a novel thermal stable polymer containing azo chromophores in the side chain. Dyes Pigments 2008;77:223–8.

[18] Peng X, Wu T, Fan J, Wang J, Zhang S, Song F, et al. An effective minor groove binder as a red fluorescent marker for live-cell DNA imaging and quantification. Angew Chem 2011;50:4180–3.

[19] Ge J-F, Zhang Q-Q, Lu J-M, Kaiser M, Wittlin S, Brun R, et al. Synthesis of cyanine dyes and investigation of their in vitro antiprotozoal activities. MedChemComm 2012;3:1435.

[20] Wurthner F, Kaiser TE, Saha-Moller CR. J-aggregates: from serendipitous discovery to supramolecular engineering of functional dye materials. Angew Chem 2011;50:3376–410.

[21] Zhou H, Watanabe T, Mito A, Honma I, Asai K, Ishigure K, et al. High nonlinear optical coefficient ($\chi^3 = 10-7$ esu) of cyanine dye j aggregates doped silica film synthesized by a simple sol–gel method. Mater Sci Eng B. 2002;95:180–6.

[22] Tang B, Yu F, Li P, Tong L, Duan X, Xie T, et al. A near-infrared neutral ph fluorescent probe for monitoring minor ph changes: imaging in living hepg2 and hl-7702 cells. J Am Chem Soc 2009;131:3016–23.

[23] He C, Wu Y, Shi G, Duan W, Song W, Song Y. Large third-order optical nonlinearities of ultrathin films containing octacarboxylic copper phthalocyanine. Org Electron 2007;8:198–205.

[24] Ge J-F, Lu Y-T, Sun R, Zhang J, Xu Q-F, Li N-J, et al. Third-order nonlinear optical properties of symmetric phenoxazinium chlorides with resonance structures at 532 nm. Dyes Pigments 2011;91:489–94.

[25] Li H, Jin Z, Li N, Xu Q, Gu H, Lu J, et al. A small-molecule-based device for data storage and electro-optical switch applications. J Mater Chem 2011;21:5860.

[26] Macchi R, Cariati E, Marinotto D, Roberto D, Tordin E, Ugo R, et al. Stable shg from in situ grown oriented nanocrystals of [(e)-n,n-dimethylamino-n'-methylstilbazolium][p-toluenesulfonate] in a pmma film. J Mater Chem 2010;20:1885.

[27] Priimagi A, Cattaneo S, Ras RHA, Valkama S, Ikkala O, Kauranen M. Polymer–dye complexes: a facile method for high doping level and aggregation control of dye molecules. Chem Mater 2005;17:5798–802.

[28] Gao J, Cui Y, Yu J, Wang Z, Wang M, Qiu J, et al. Molecular design and synthesis of hetero-trichromophore for enhanced nonlinear optical activity. Macromolecules 2009;42:2198–203.

[29] Zhu Y-J, Qin A-J, Fu L-M, Ai X-C, Guo Z-X, Zhang J-P, et al. Syntheses of novel 1,3-diazaazulene derivatives and their nonlinear optical characterization. J Mater Chem 2007;17:2101.

[30] Cui F, Feng C, Xie R, Hua Z, Cui X, Zhou J, et al. Significant third-order optical nonlinearity enhancement of gold nanoparticle incorporated mesoporous silica thin films by magnetic field thermal treatment. J Mater Chem 2010;20:8399.

[31] Cherioux F, Audebert P, Maillotte H, Zyss J. Synthesis and characterisation of an octupolar polymer and new molecular octupoles with off-resonant third order optical nonlinearities. Chem Commun 1999;0:2083–4.

[32] Lee S, Becht GA, Lee B, Burns CT, Firestone MA. Electropolymerization of a bifunctional ionic liquid monomer yields an electroactive liquid-crystalline polymer. Adv Funct Mater 2010;20:2063–70.

[33] Kim HK, Kang S-J, Choi S-K, Min Y-H, Yoon C-S. Highly efficient organic/inorganic hybrid nonlinear optic materials via sol–gel process: synthesis, optical properties, and photobleaching for channel waveguides. Chem Mater 1999;11:779–88.

[34] Hucknall A, Kim D-H, Rangarajan S, Hill RT, Reichert WM, Chilkoti A. Simple fabrication of antibody microarrays on nonfouling polymer brushes with femtomolar sensitivity for protein analytes in serum and blood. Adv Mater 2009;21:1968–71.

[35] Sun R, Yan B-L, Ge J-F, Xu Q-f, Li N-J, Wu X-Z, et al. Third-order nonlinear optical properties of unsymmetric pentamethine cyanine dyes possessing benzoxazolyl and benzothiazolyl groups. Dyes Pigments 2013;96:189–95.

[36] Gadde S, Batchelor EK, Weiss JP, Ling Y, Kaifer AE. Control of h- and j-aggregate formation via host–guest complexation using cucurbituril hosts. J Am Chem Soc 2008;130:17114–9.

[37] Frisch MJ, Trucks GW, Schlegel HB, Scuseria GE, Robb MA, Cheeseman JR, et al. Gaussian 09, revision b.01. Wallingford CT: Gaussian, Inc.; 2010.